

# On the connection of radio and $\gamma$ -ray emission of blazars

## Abstract

Blazars are a sub-category of radio-loud Active Galactic Nuclei having their jet pointing towards us and are known for their emission covering practically all frequencies of the electromagnetic spectrum. These sources, in some cases, exhibit a correlation between gamma-ray and radio emission, especially during flaring episodes. Adopting the hypothesis that high energy photons are emitted by relativistic electrons close to the central black hole, we study the evolution of this population of particles as they move down the jet and lose energy by radiation and adiabatic expansion. In this scenario, gamma-rays are produced early on, when the electrons are still very energetic, while radio emission at a later time when the electrons have cooled and the emission region becomes optically thin to synchrotron self-absorption due to expansion. We calculate the emitted spectrum by solving the kinetic equations of particles and photons using a numerical code which takes into account the expansion of the source. We will discuss the parameters entering our calculations (like the magnetic field strength, the density of relativistic electrons, etc) in connection to the observational data.

## What is an Active Galactic Nucleus (AGN)?

### The basic observational properties of AGN:

- ▶ Extremely bright nucleus
- ▶ Relativistic outflows (jets)
- ▶ Multiwavelength emission (from radio to  $\gamma$ -rays)
- ▶ Emission lines
- ▶ Polarization

### The anatomy of AGN:

- ▶ A supermassive black hole
- ▶ Accretion disk
- ▶ Torus
- ▶ Bipolar relativistic jets
- ▶ Clouds with broad and narrow emission lines

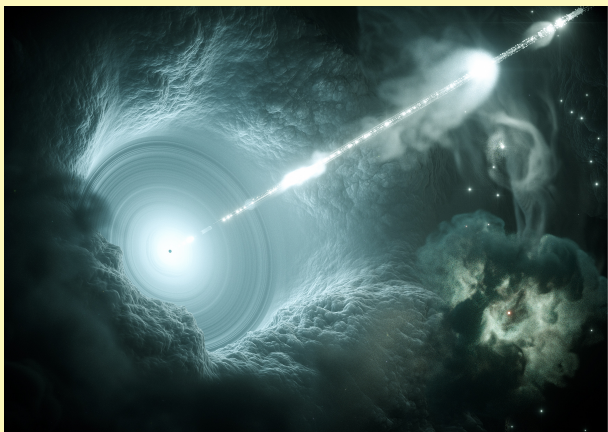


Figure: An illustration of an AGN. Credit: DESY

## Blazars

Blazars are the most extreme sub-category of Active Galactic Nuclei. Their emission is coming from a relativistic jet pointing toward the Earth. They are rapidly variable, strong  $\gamma$ -ray emitters and radio and optical polarized sources. Blazars are divided into two categories:

- ▶ BL Lac objects with weak emission lines
- ▶ Flat Spectrum Radio Quasars (FSRQs) with strong emission lines

## Spectral Energy Distribution (SED)

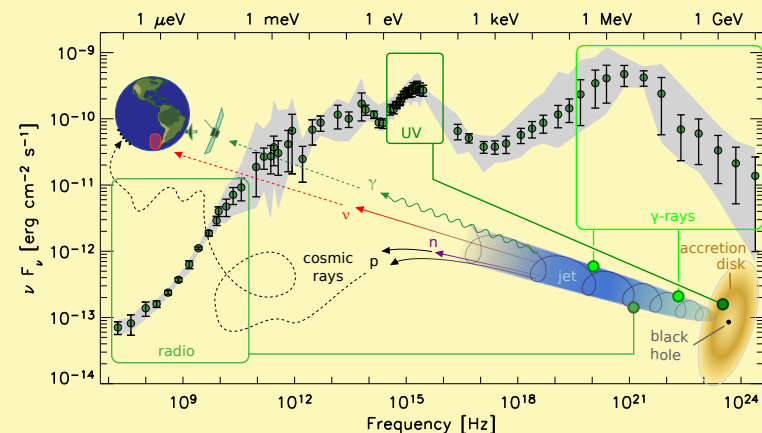


Figure: One of the characteristic features of blazar jet emission is the shape of its spectral energy distribution (SED), which usually has two components: a low-energy component extending from radio to UV/soft X-rays and a high-energy component lying between hard X rays and TeV  $\gamma$  rays. Image credit: [3]

## Motivation of this work

- ▶ Localization of emission
- ▶ Correlations of Multiwavelength flares

# On the connection of radio and $\gamma$ -ray emission of blazars

## Model Setup

The characteristics of our model are:

- ▶ An emitting region (a blob of radiative relativistic electrons) which expands with an expanding velocity  $u_{exp}$ .
- ▶ The blob of plasma is assumed to be spherical with radius  $R(t) = R_0 + u_{exp}t$  in its comoving frame (where  $R_0$  is the initial radius of the source) and moves with highly relativistic speed  $\beta c$ , giving it a Lorentz factor  $\Gamma = (1 - \beta^2)^{-1/2}$ . The jet makes an angle to our line of sight  $\theta$ , thus the relativistic Doppler factor is  $\delta = [\Gamma(1 - \beta \cos \theta)]^{-1}$ .
- ▶ The magnetic field has the strength  $B = B_0 \left(\frac{R_0}{R}\right)^s$ , where  $B_0$  is the initial value of the magnetic field and  $s$  is a free parameter.
- ▶ Relativistic electrons with a power law distribution are injected ( $Q_e$ ). The electrons luminosity are related to  $Q_e$  by  $L_e^{inj} = m_e c^2 \int_{\gamma_{min}}^{\gamma_{max}} Q_e(\gamma, t) \gamma d\gamma$  where
 
$$Q_e(\gamma, R) = q_e(R(t)) \gamma^{-p} = q_{e0} \left(\frac{R_0}{R(t)}\right)^\chi \gamma^{-p}, \quad \gamma_{min} \leq \gamma \leq \gamma_{max},$$
 where  $\chi$  can be positive or negative, and  $\gamma_{min}$ ,  $\gamma_{max}$  are, respectively, the minimum and maximum Lorentz factors of the electron distribution..
- ▶ The characteristic time scale of the problem is the initial crossing time of the source,  $t_{cross} = \frac{R_0}{c}$ .

## Physical Processes

The relativistic electrons interact and radiate through the following processes:

- ▶ **Synchrotron radiation**
- ▶ **Inverse Compton Scattering**
- ▶ **Photon-photon absorption**
- ▶ **Synchrotron self-absorption**
- ▶ **Adiabatic losses**

## Numerical Approach

We developed a numerical code, based on [2] in order to calculate the temporal evolution of the electrons and photons distribution function. This code solves two integro-differential equations, each describing the losses/sinks ( $\mathcal{L}$ ) and injection of relativistic electrons ( $Q_e$ ) and photons in the emitting region. The kinetic equation of electrons reads:

$$\frac{\partial N(\gamma, t)}{\partial t} + \sum \mathcal{L}_i N(\gamma, t) = Q_e(\gamma, t),$$

$$\sum \mathcal{L}_i = \frac{\partial}{\partial \gamma} [(A_{syn}(\gamma, t) + A_{ICS}(\gamma, t) + A_{exp}(\gamma, t))]$$

where the terms  $A_{syn}$ ,  $A_{ICS}$ ,  $A_{exp}$  are the loss rates for synchrotron emission, inverse Compton scattering, and adiabatic expansion respectively.

## The role of synchrotron self-absorption

The frequency below which the synchrotron radiation is absorbed can be derived by the condition  $\alpha_{\nu_{ssa}} R(t) \sim 1$  where  $\alpha_{\nu_{ssa}}(t)$  is the absorption coefficient (e.g. [4]). The synchrotron self-absorption frequency  $\nu_{ssa}$  is a function of blob radius through its dependence on the magnetic field and electron number density. A blob at small distances from the jet base is optically thick to synchrotron radiation, but it becomes optically thin as it expands and moves to further distances.

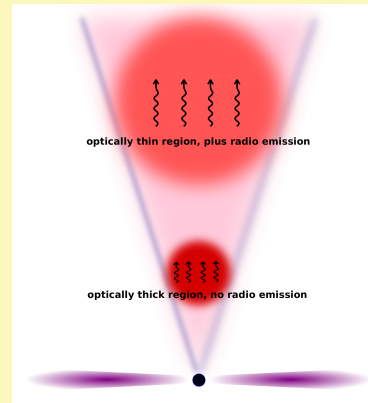


**Figure:** A sketch of our model. High energy emission is produced close to the central engine; on the other hand, radio frequencies are absorbed. The source becomes optically thin at further distances.

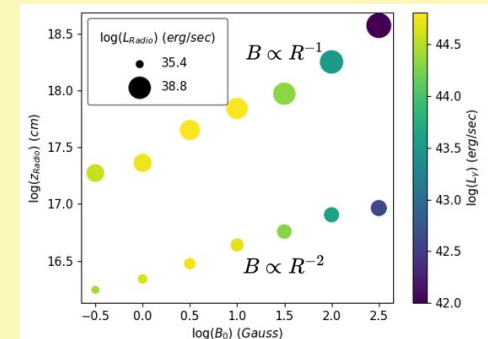


**Figure:** The dependence on initial magnetic field value of the distance where the radio frequencies escape. The figure depicts two different radius profiles. Also, the  $\gamma$ -ray (at the base of the jet) and radio luminosity (at the distance where the source is optically thin) are represented. The other parameters have the values:  $R_0 = 10^{15}$  cm,  $L_{e0}^{inj} = 10^{42}$  erg s $^{-1}$ ,  $u_{exp} = 0.1 c$ ,  $\gamma_{min} = 1$ ,  $\gamma_{max} = 10^6$ ,  $p = 2$ ,  $\delta = 10$  and  $z_{init} = 0.01$  pc.

## Steady State Emission

1. We assume that blobs with the same initial properties are continuously created at a distance  $z_0$  from the central engine. This is equivalent to a conical flow with a half-opening angle  $\phi = \arctan(R_0/z_0)$ . The distance  $z$  traveled by a blob since its "birth", as measured in the black hole's rest frame, is related to its radius  $R$  as:  $z(t) = z_0 + \beta c(R(t) - R_0)/\Gamma u_{exp}$ .
2. We integrate along the line of sight the SED in order to reproduce the total steady-state spectrum of the source which is observed.
3. We compare our results with the observational data of the source Mrk421.

# On the connection of radio and $\gamma$ -ray emission of blazars

## The structure of a blazar SED

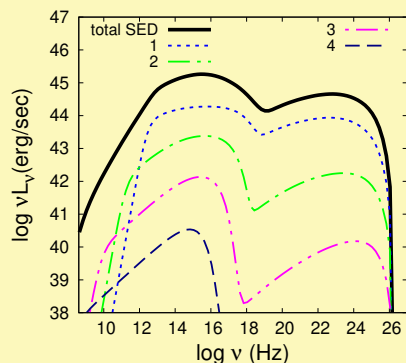


**Figure:** Steady-state SED of a fiducial BL Lac source (thick black line), computed by superimposing the emission of  $10^4$  blobs that are produced continuously at distance  $z_0 = 10^{-3}$  pc from the central engine. For illustrative purposes, we present the spectra of a few indicative blobs (1 :  $R_1 = 10^{15.5}$  cm,  $z_1 = 1.6 \times 10^{-3}$  pc; 2 :  $R_2 = 10^{16.5}$  cm,  $z_2 = 7 \times 10^{-3}$  pc; 3 :  $R_3 = 10^{17.5}$  cm,  $z_3 = 6 \times 10^{-2}$  pc; 4 :  $R_4 = 10^{18.5}$  cm,  $z_4 = z_{final} = 6 \times 10^{-1}$  pc). All blobs are initialized with the same parameters:  $B_0 = 10$  G,  $R_0 = 10^{15}$  cm,  $L_{e_0}^{inj} = 10^{42}$  erg  $s^{-1}$ ,  $u_{exp} = 0.3$  c,  $\gamma_{min} = 1$ ,  $\gamma_{max} = 10^5$ ,  $p = 2$ ,  $\Gamma = 5$  and  $\delta = 10$ . The magnetic field and electron injection luminosity decrease linearly with radius ( $s, \chi = 1$ ) [1].

## Mrk 421 steady state emission

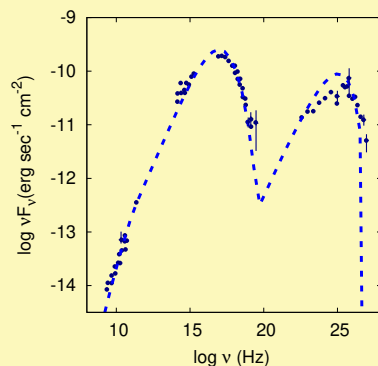


**Figure:** Steady-state SED of a fiducial BL Lac source (thick black line), computed by superimposing the emission of  $10^3$  blobs that are produced continuously at distance  $z_0 = 10^{-2}$  pc from the central engine. All blobs are initialized with the same parameters:  $B_0 = 0.3$  G,  $R_0 = 10^{16}$  cm,  $L_{e_0}^{inj} = 3 \times 10^{41}$  erg  $s^{-1}$ ,  $u_{exp} = 0.2$  c,  $\gamma_{min} = 1$ ,  $\gamma_{max} = 10^6$ ,  $p = 2$ ,  $\delta = 10$ . The magnetic field and electron injection luminosity decrease linearly with radius ( $s, \chi = 1$ ).

## Flaring Episodes

We assume a re-acceleration episode in a distance  $z$  from the central engine. The injected electrons distribution has the form:

$$Q_e(\gamma, R) = q_e(R(t))\gamma^{-p} \left( 1 + \frac{(\alpha - 1)w^2}{4(t - t_0)^2 + w^2} \right) = q_{e_0} \left( \frac{R_0}{R(t)} \right)^\chi \gamma^{-p} \left( 1 + \frac{(\alpha - 1)w^2}{4(t - t_0)^2 + w^2} \right), \quad \gamma_{min} \leq \gamma \leq \gamma_{max}$$

where  $\alpha$  is the value at maximum,  $w$  the width of the injection and  $t_0$  the time when the maximum is injected.

These flaring episodes - depending on the set of parameters- reproduce symmetrical and extended flares.

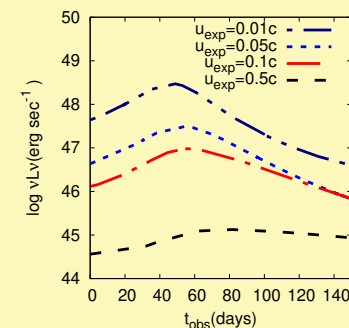


**Figure:** The dependence of the symmetry of the pulses on the expanding velocity. In the case of high values of the  $u_{exp}$  the decay time is larger than the rise one (extended flare).

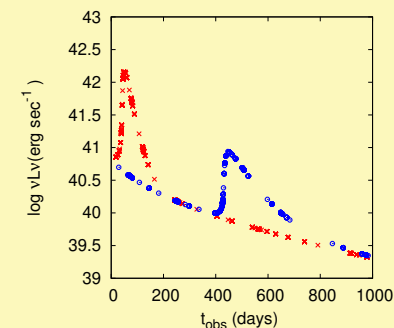
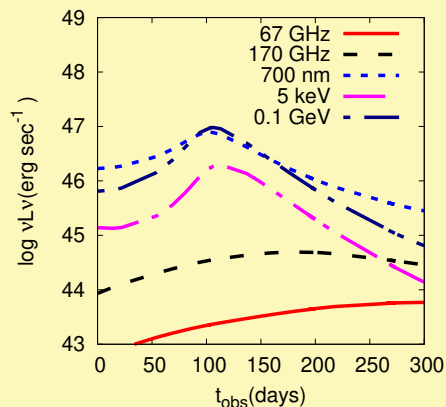


**Figure:** The flare which occurs earlier (red line) is dominated by strong cooling losses, and it appears more symmetrical, contrary to the later one (blue line), which is dominated by the adiabatic losses.

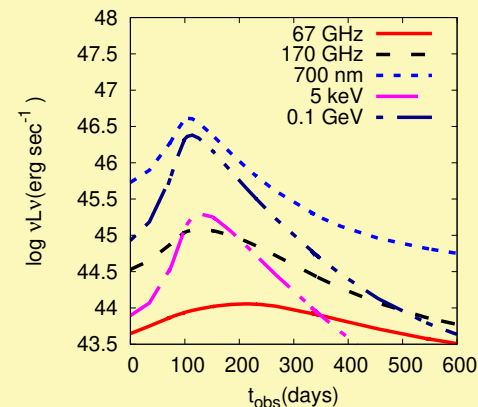
# On the connection of radio and $\gamma$ -ray emission of blazars

## Multiwavelength Correlations

In order to investigate the multiwavelength correlations, we assume a re-acceleration episode occurring at different distances from the central engine. Here we present an example: the width of the injection is  $w = 100 t_{cross}$  and the value at the maximum is  $\alpha = 100$  larger than the bulk flow. The initial values of the bulk flow are:  $B_0 = 10$  G,  $R_0 = 10^{16}$  cm,  $L_{e_0}^{inj} = 10^{44}$  erg  $s^{-1}$ ,  $u_{exp} = 0.1$  c,  $\gamma_{min} = 1$ ,  $\gamma_{max} = 10^5$ ,  $p = 2$   $\delta = 10$  and the profiles of the magnetic field strength and electrons luminosity are decreasing linearly with the time. Relativistic electrons are injected at  $z_1 = 1$  pc (left panel) and at  $z_2 = 10$  pc (right panel). In the first case, the radio frequencies are absorbed, however it seems that 170 GHz photons are marginally absorbed. In the second case, all the photons escape.



**Figure:** A flare in an optically thick region. The time lag between  $\gamma$  and X rays is 7 days; and the optical peak is observed 1 day earlier than  $\gamma$ -rays one.

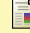





**Figure:** A flare in an optically thin region. The optical peak is preceding 5 days earlier than  $\gamma$ -rays one, while the time lag between  $\gamma$  and X rays is 13 days, between  $\gamma$ -rays and 170 GHz is 16 days and  $\gamma$ -rays and 67 GHz is 77 days.

## Conclusions

- ▶ Development of a new one-zone expanding numerical leptonic code.
- ▶ Prediction of the localization of radio emission depending on the basic physical quantities of the source.
- ▶ Flares in radio and  $\gamma$ -rays may be produced by re-acceleration of electrons at a large distance from the central engine.
- ▶ Close to the central engine radio flares could not be produced.

## References

-  S. Boula, M. Petropoulou, and A. Mastichiadis. On the Connection of Radio and  $\gamma$ -Ray Emission in Blazars. *Galaxies*, 7(1):3, Dec. 2018.
-  A. Mastichiadis and J. G. Kirk. Self-consistent particle acceleration in active galactic nuclei. , 295:613, Mar. 1995.
-  B. Rani, M. Petropoulou, H. Zhang, F. D'Ammando, J. Finke, M. Baring, M. Boettcher, S. Dimitrakoudis, Z. Gan, D. Giannios, D. H. Hartmann, T. P. Krichbaum, A. P. Marscher, A. Mastichiadis, K. Nalewajko, R. Ojha, D. Paneque, C. Shrader, L. Sironi, A. Tchekhovskoy, D. J. Thompson, N. Vlahakis, and T. M. Venters. Multi-Physics of AGN Jets in the Multi-Messenger Era. , 51(3):92, May 2019.
-  G. B. Rybicki and A. P. Lightman. *Radiative processes in astrophysics*. 1979.